THREE-AXIS AIR-BEARING BASED PLATFORM FOR SMALL SATELLITE ATTITUDE DETERMINATION AND CONTROL SIMULATION.

J. Prado[1]., G. Bisiacchi[2]., L. Reyes[3]., E. Vicente[4]., F. Contreras[1]., M. Mesinas[1]., and A. Juárez[1].

[1]Instituto de Geografía, UNAM. Circ. Ext. Cd. Universitaria, Coyoacán 04510. México D.F. México.
[2]Centro Tecnológico Aragón, Av. Rancho seco S/N col. Impulsora, Cd. Nezahualcóyotl 57130, Edo. Mex. México.
[3]Instituto Mexicano del Transporte, Km.12+000 Carr. Querétaro-Galindo Sanfandila, Pedro Escobedo,Qro. C.P.76700.
[4]Instituto de Ingeniería, UNAM, Cd. Universitaria Coyoacán, 04510, México D.F. México.
jprado@igg.unam.mx, pdruan@yahoo.com.mx, luis.reyes@imt.mx, evv@servidor.unam.mx

Received: April 28TH, 2005. Accepted:August 23TH, 2005

ABSTRACT

A frictionless environment simulation platform, utilized for accomplishing three-axis attitude control tests in small satellites, is introduced. It is employed to develop, improve, and carry out objective tests of sensors, actuators, and algorithms in the experimental framework. Different sensors (i.e. sun, earth, magnetometer, and an inertial measurement unit) are utilized to assess three-axis deviations. A set of three inertial wheels is used as primary actuators for attitude control, together with three mutually perpendicular magnetic coils intended for desaturation purposes, and as a backup control system. Accurate balancing, through the platform's center of mass relocation into the geometrical center of the spherical air-bearing, significatively reduces gravitational torques, generating a virtually torque-free environment. A very practical balancing procedure was developed for equilibrating the table in the local horizontal plane, with a reduced final residual torque. A wireless monitoring system was developed for on-line and post-processing analysis; attitude data are displayed and stored, allowing properly evaluate the sensors, actuators, and algorithms. A specifically designed onboard computer and a set of microcontrollers are used to carry out attitude determination and control tasks in a distributed control scheme.

The main components and subsystems of the simulation platform are described in detail.

RESUMEN

Se presenta una plataforma de simulación de un medio sin fricción, utilizada para llevar a cabo pruebas de control de orientación en satélites pequeños. Ésta se emplea para efectuar de una manera objetiva, el desarrollo, mejoramiento y pruebas de funcionamiento de: sensores, actuadores y algoritmos; desde un punto de vista experimental. Se utilizan diferentes sensores (i.e. sol, tierra, magnetómetro y unidad de medición inercial) para determinar su desviación en tres ejes. Tres ruedas inerciales constituyen el grupo de actuadores primarios para control de orientación, trabajando en conjunto con tres bobinas magnéticas, mutuamente perpendiculares, que sirven para desaturar las ruedas y también como sistema de control de respaldo. La ejecución de un balanceo exacto, a través de la re-localización del centro de masa de la plataforma sobre el centro geométrico del balero de aire esférico, reduce significativamente los pares gravitacionales, generando un medio virtualmente libre de pares externos. Se desarrolló un procedimiento muy práctico de balanceo, para equilibrar la mesa en el plano horizontal local, logrando obtener un par residual final pequeño. Un sistema de monitoreo inalámbrico fue desarrollado con el propósito de llevar a cabo un análisis en línea y en post-proceso; los datos de orientación son desplegados y almacenados, permitiendo una correcta evaluación de sensores, actuadores y algoritmos. Una computadora a bordo de diseño específico y un conjunto de microcontroladores, llevan a cabo tareas de detección, orientación y control, en un esquema de control distribuido.

Se describen con detalle los principales componentes y subsistemas de la plataforma de simulación.

Keywords: Frictionless Environment Simulator, Automatic Static Balancing, Sliding Masses, Spacecraft Simulator, Spherical Air-Bearing, Wireless Monitoring System.

1.INTRODUCTION

Attitude determination and control systems onboard small satellites increase significantly the amount and quality of the experiments that can be accomplished on Earth's orbit. Future small satellites will have an unprecedented degree of complexity and pointing accuracy. Autonomous on-board processing capabilities and high speed are imperative for the new demanding tasks, such as: optical communications [1], formation flying [2], and interferometer missions [3].

Innovative control techniques fulfill the new stringent requirements, however, experimental validation is a very important aspect that has been missed in the last years in attitude determination and control stabilization [4]. Physical simulation is very helpful, particularly when novel control laws will be incorporated into next-generation spacecraft [4]. Nevertheless, reproducing the whole characteristics of the space environment on Earth is practically impossible. Simulation in laboratory is restricted, in most of the cases, to torque-free movement with systems varying from 1 to 3 degrees-of-freedom, and also; a combination of rotational motion and force-free translational motion (i.e. four degrees of freedom) can be achieved [5]. Very limited experimentation can be carried-out with zero-g in adapted aircrafts that can fly in a parabolic path, reproducing a weightless condition from 23 to 26 s, meanwhile a drop tower can provide from 2.2 to 3.3 s of microgravity. Thermo-vacuum chambers are used to simulate thermal cycles at a very low pressure, and magnetic simulators [6] can provide the three vectorial components the satellite encounters during its orbital fly.

Air-bearing offers a nearly torque-free environment, perhaps as close as possible to that of the space, for this reason it is the preferred technology for ground-based research in space dynamics, attitude, and control [7], however, it certainly cannot provide the full experience of microgravity. In nearly 46 years of development, facilities widely vary, ranging from very sophisticated government laboratories, to less expensive university testbeds [7].

Several academic institutions have constructed physical simulators with the purpose to educate the next generation of attitude dynamics and control engineers [4, 8]. This paper describes a spacecraft simulator, based on a spherical air-bearing, developed at the Alternative Remote Sensing and Advanced Technology Laboratory of the Institute of Geography, UNAM [9]. This equipment is being used to develop, improve, and carry out tests of sensors, actuators, and algorithms in the experimental framework.

Platform balancing is one of the most important issues that must be considered before testing. Accurate balancing, through the platform's center of mass relocation into the geometrical center of the spherical air-bearing, significantly reduces the external gravitational torques, generating thus a virtually torque-free environment. Moreover, the quality of the experiments is in close relationship with the precision reached during the balancing process [8]. It can be readily figure out that cable usage will cause considerable unbalances; information can only be transmitted in or out by radio links [10]. We compare two different balancing techniques and report the results at the end of the document.

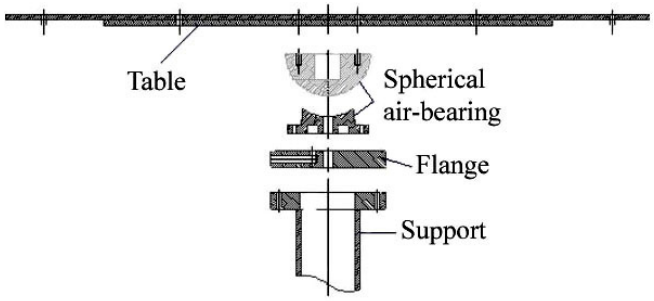

Figure 1. Frictionless environment simulation platform

2. SYSTEM OVERVIEW

The basic design concept of the simulator (see Figs. 1 & 2), consists of a platform suspended on a spherical air-bearing [10]. The table contains sensors, actuators, a bi-directional radio link, a balancing system, and an onboard computer. Three wheels are the primary actuator units, and can operate in either: reaction or momentum wheel mode. DC motors drive them, and their speed controlled by PLL circuits. Three mutually perpendicular magnetic coils are used for desaturating the momentum wheels, and also employed as a backup control system. Power is provided by different battery sets, basically grouped by

voltage and power capacity. Regulated dc/dc converters supply very stable voltages that delicate inertial measuring sensors require. An automatic balancing system relocates the center of mass into the geometrical center of the air-bearing. The on-board computer is devoted to data acquisition, filtering, and algorithm execution. Through wireless communication, a remote desktop PC displays and stores the deviation angles the platform undergoes during balancing, or control maneuvering experimentation.

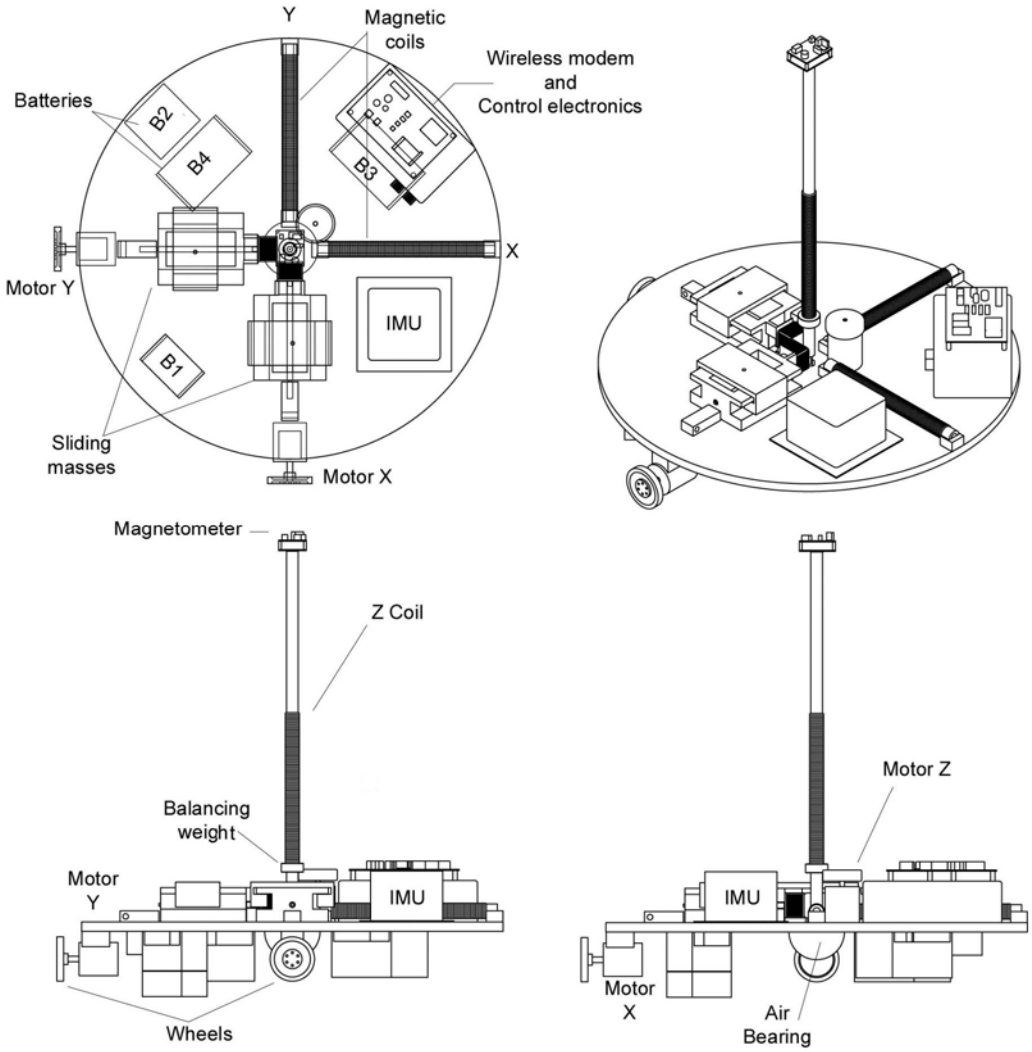

Figure 2. Simulation platform schematic drawings

3. MAIN COMPONENTS AND SUBSYSTEM DESCRIPTION

3.1 Table

The table is round-shaped with an external diameter of 76 cm, and 17 mm thick. It was constructed with a PVC foam sheet, sandwiched by three layers of bi-axial carbon-fiber fabric and embedded into a matrix of epoxy resin. Composites will permit residual torques been diminished, as will be discussed later; carbon-fiber has an extremely high stiffness-to-weight ratio with a thermal expansion coefficient of 0.028 x 10-6 cm/cm • C, meanwhile aluminum has a value of 25 x 10-6 cm/cm • C.

3.2 Spherical air-bearing.

The spherical air-bearing was designed and constructed in-house [11], and machined in phosphor bronze with a nominal load capacity of 80 kg. Between the semi-sphere and the cup (see Fig. 3), a thin air film (.0254 mm thick) is produced. It is of the multiflow type, with six jets (0.55 mm diameter) proportionally spaced. The final size of the semi-sphere was 99.9348 ± 0.0414 mm, meanwhile the cup had a diameter of 100.4727 ± 0.0235 mm. It has movements of 360º in Yaw, and ±50º in Roll and Pitch; which is satisfactory for our purposes. Work pressure of the external source of compressed air, varies with the load

capacity, typical values are around 3.2 kg/cm2 with a payload of 35 kg. Air filters are mandatory because moisture, oil, or dust can break the thin air cushion.

Figure 3. Semi-sphere and cup, main components of the spherical air-bearing

3.3 Attitude Sensors

A set of different attitude sensors is used to establish platform deviations. Particularly, gyros are used to directly measure angular rates (for control law implementation), and together with the accelerometers, have the commandment to determine the center of mass, and the inertia matrix of the system.

3.3.1. *Inertial measurement unit (IMU)*

A combination of low-cost solid-state gyroscopes and accelerometers were integrated to conform the IMU (Fig. 4). Gyro drift limits the utilization of the IMU to short-term experimentation (i.e. some minutes). Micromachined accelerometers [12] with an operational range of ± 2 G's, RMS noise level of 0.02 g were used. The gyroscopes [13] are piezoelectric devices with an operational interval of ± 100 o/s and RMS noise level of 0.05 o/s. Butterworth second-order low-pass filters, for signal conditioning and noise reduction, were connected in series with these devices

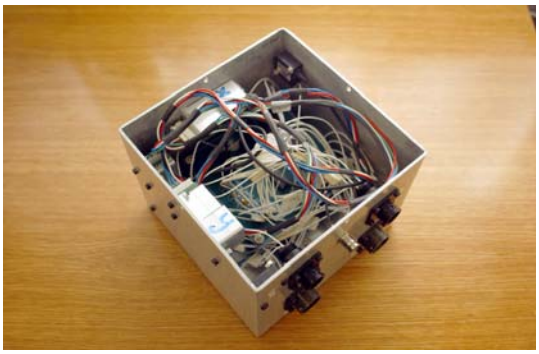

Figure 4. IMU containing the inertial sensors and the circuits for signal conditioning and filtering

3.3.2 *Three-axis magnetometer*

An electronic compass [14], with two attached inclinometers, is the sensor employed to obtain the three vectorial components of the Earth's magnetic field. This device outputs continuous azimuth (accuracy is ≤ 0.5 arc-deg), the three components of the magnetic field, dual axis tilt (for up to ± 80 arc-deg with an accuracy of 0.25 arc-deg), and temperature data. Serial communication is carried out through an RS232 interface. The inclinometers are used in one of the automatic balancing procedures that will be discussed later

3.3.3 *Sun sensor*

This analog device provides independent orientation in two-axis, using four photocells in a cross-shaped arrangement (Fig. 5). A conditioning circuit amplifies and subtracts the signals of the two cells of the corresponding axe, determining the deviation from the Sun. Accuracy obtained is ± 0.1 arc-deg and angle coverage can be adjusted between ± 12 and ± 25 arc-deg, varying

the window's height. One version of this sensor was manufactured with space-rated components and calibrated for its operation in small-satellites [15].

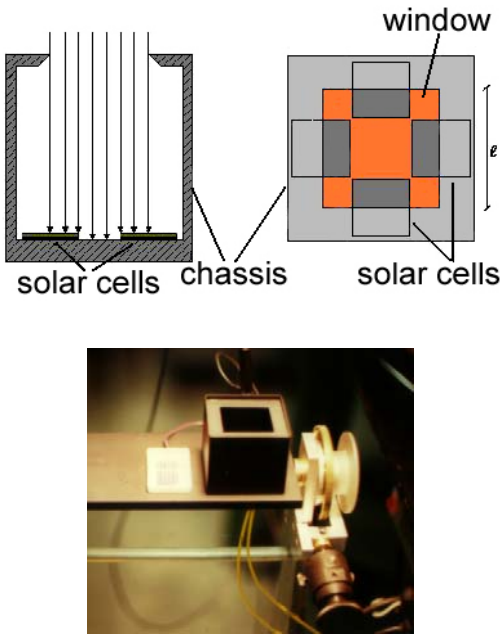

Figure 5. Schematic diagram of the sun sensor, and calibration test

3.3.4 *Earth sensor*

A set of four static Earth sensors is used to determine the attitude in two independent axis of the platform (Fig. 6). Lead selenide detectors were employed [16] with a spectral response ranging between 1 and 5 μm. Laboratory test with these sensors, using a hot aluminium plate as an Earth simulator, allowed us to get a resolution of ± 0.5 arc-deg [17]. Analog signals coming from the detectors passes through a conditioning circuit, then a Sallen-Key filter for noise reduction, and finally are directed to the on-board computer, for attitude determination.

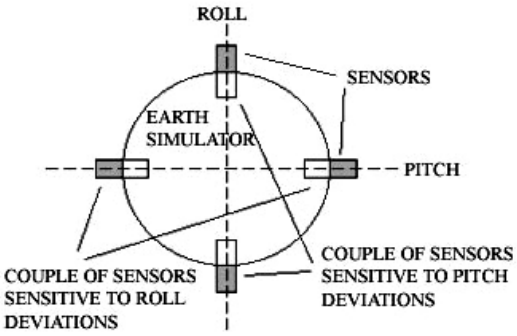

Figure 6. Earth sensors' arrangement for two-axis attitude determination

3.4 Momentum/reaction wheels

In order to carry out laboratory tests, direct current motors were used to drive the inertial wheels, instead of expensive space-rated momentum/reaction components. Three TEAC® DC motors with a 24 V nominal voltage @ 0.1 A were employed as actuators, jointly with three wheels made out of bronze. In momentum wheel mode the speed of the DC motors varies between 1,400 and 2,200 rpm, being the maximum speed limit 4,200 rpm. A PLL maintains a constant speed, and a tachometer is utilized to directly measure the angular velocity [18]. Encoders were considered for the same purpose, and discarded because of time delays.

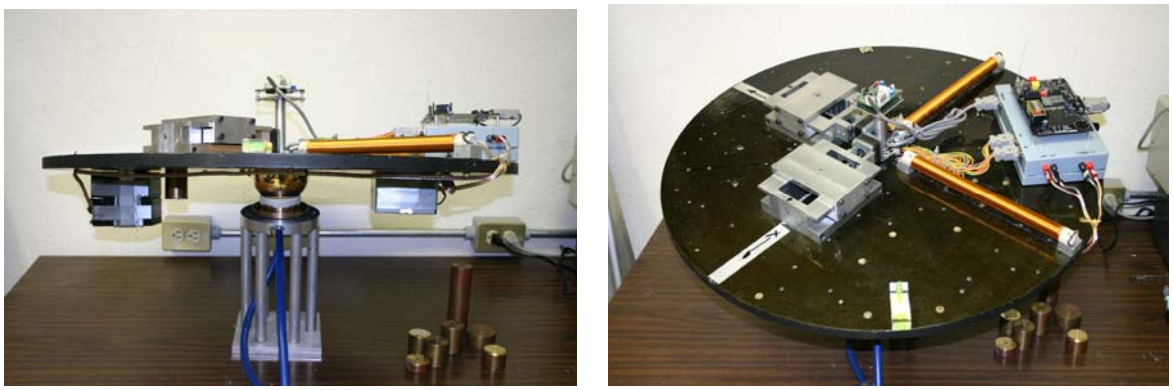

Figure 7. The spacecraft simulator with the two-axis balancing system, the electronic compass, a microcontroller and two magnetic coils

3.5 Magnetic coils

Control systems with magnetic coils can be effectively used to carry out pointing maneuvers and attitude stabilization at any Terrestrial orbit, including the geosynchronous located at 36,000 km of height [19]. Magnetic control systems are low weight, don't have moving parts, and are relatively simple. Additionally, non-sophisticated sensors, neither consumables on board, are needed. Magnetic torque is very attractive for space applications, however, the final pointing accuracy is limited to ± 3 arc-deg and the strength of the control torque depends on the magnitude of the three vectorial components of the magnetic field in the particular location of the orbit, the maneuver will be performed. An autonomous navigation system could be implemented in orbit using a magnetometer and a geomagnetic field model, increasing significatively the onboard capabilities of the spacecraft [20]. Tubular magnetic coils with ferromagnetic core were designed and constructed (see Fig. 7), with a nominal torque capacity of 12 A-m2 [21]. Some limited experimentation with very simple control maneuvers were carried out in the laboratory [22], due to the unavailability of an Earth magnetic field simulator

3.6 Wireless communication and monitoring system

The communication between the platform and the PC, where attitude data are stored and displayed, is accomplished by a bidirectional radio link. Cable usage is not acceptable in this frictionless media, because balancing can easily get out of allowable limits. Transmitter/receiver modules (Linx Technologies® [23]) were used to solve the problem of wireless communication between the platform and the ground station computer. These devices offer the possibility of handling analog or digital data, the RS232 protocol, eight channels in the range of 902 to 928 MHz, and an operating distance of 100 m using FSK modulation/demodulation.

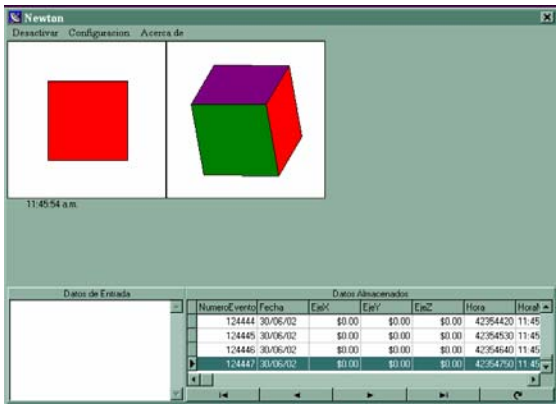

Figure 8. Monitoring system main screen

A monitoring system was developed [24] for supervising platform's movements during balancing and attitude control tests. Specifically designed electronics and software are used to transmit, display and store the evolution of the platform's orientation during the essays. For attitude determination and control assessment, it is imperative to store the evolution of the simulator's attitude. The software displays in real time: two perspectives of the platform's orientation, three-axis deviation

angles, and the internal clock. All these data are received through the wireless interface. Attitude information is saved in a user's defined data file. Fig. 8 shows the graphics and data displayed by the monitoring system.

3.7 On-board computer

In early stages of the development of the spacecraft simulator, MC68HC11microcontrollers [25] were used to carry out: filtering, attitude determination, and control tasks. The last version of this simulator was used in a specifically designed onboard computer (OC) [26]. It constitutes a heritage from the flight computer (FC) developed for the Satex microsatellite project, which included a main single processing board, and two cold standby spares. As a matter of fact the OC represent one of those FC's single processing boards. It contains a 16-bit SAB80C166 RISC microcontroller, with four-stage pipeline, 10 channels of 10-bit for A/D conversion, five timers/counters, three serial channels, a watchdog timer, an interrupt system, and 76 I/O lines. The board also integrates 64 KB of ROM and 1.28 MB of SRAM protected by a TEMIC 29C516E error detection and correction unit. Every integrated circuit, except the RISC microcontroller and memory, are military components (MIL-STD-883). The OC contains enough hardware resources to automate all the spacecraft simulator operations. Fig. 9 depicts the components connection around the OC.

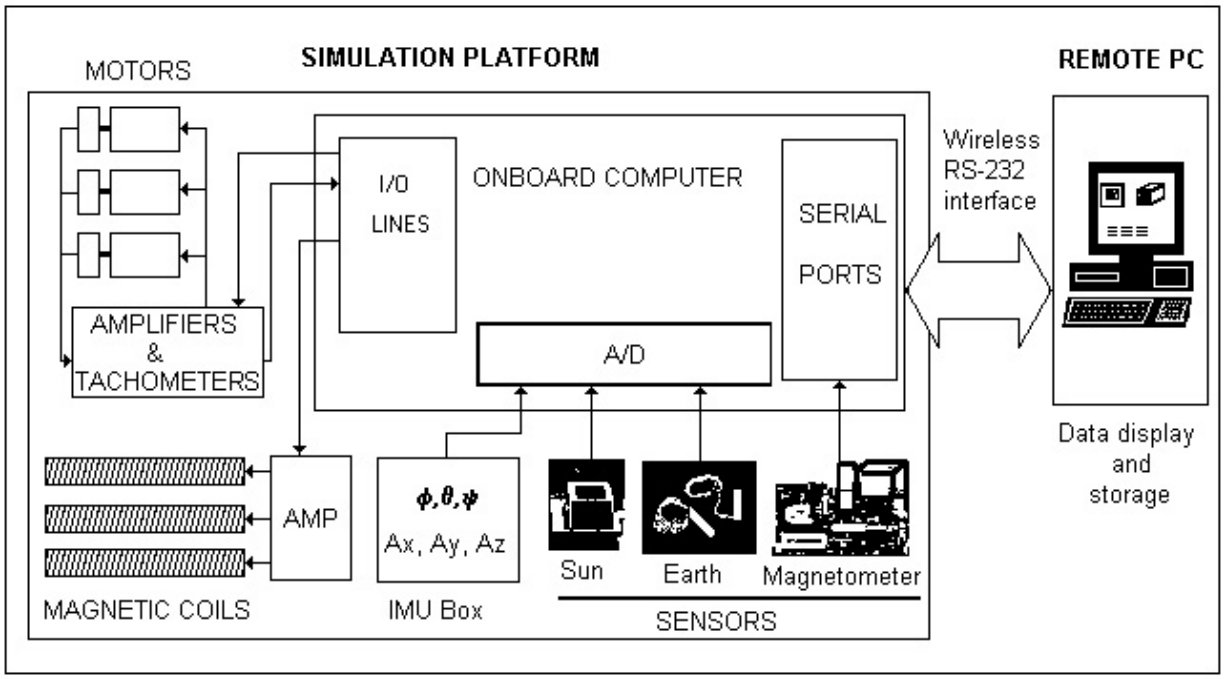

Figure 9. Overview of the simulator's component interconnection

4. BALANCING SYSTEM

As mentioned before, the balancing procedure is a very important issue that will permit gravitational torques to be diminished into the spacecraft simulator. The balancing process is particularly tedious and difficult to carry out due to the geometrical complexity of some of the components [27] (e.g. cable harness, etc.). An unbalance exists when the center of gravity (CG) and/or the principal inertia axis, have a shift with respect to the rotational axis [28]. Lang [29] has demonstrated that for statically balancing a system (i.e. positioning its center of mass) a single mass is needed. In order to dynamically balancing a system (i.e. positioning of the principal inertia axis) two masses are needed, either, added or subtracted. To fully characterize the system for dynamic balancing or control purposes it is necessary to have: the total mass of the system, the inertia matrix, the platform's attitude, and a dynamical model. One way of calculating the moments of inertia (MOI) of the platform is to use a CAD model, and assigning mass densities to the components [4]. The analytical approach uses the mass, the geometrical shape, and the X, Y, Z location of each component in body-fixed coordinates to compute the MOI. The traditional pendulum method takes measurements of the oscillating period of the system and determines its inertial properties [27]. All of these methods give a good estimate of the inertia matrix with an accuracy of around 5 per cent of the real value. Another experimental method measures the external reaction forces induced by load cells and find the inertia matrix that best fits the equations of motion following a least-squares approach [30], with the disadvantage of involving an important effort during

setting up and experimentation. Another way to determine inertial properties is from observations, using rate and acceleration sensors, together with a LMS technique [31].

In the next paragraphs we describe the two approaches developed to balance the simulator. In the first, the matrix of inertia and the center of mass are estimated through system's identification by angular velocity and acceleration sensors, and solving a set of Euler's equations of motion for a rigid body. A set of three sliding masses was employed as actuators for center of mass relocation in three-axis [32]. In the second method, a very important modification was implemented, performing only a two-axis (roll & pitch) balancing, making use of the signals of two inclinometers for local horizontal determination, and two sliding masses for center of mass repositioning [33]. This last approach allows considerable savings in mass, size, complexity, and represents an important accuracy improvement, as will be discussed later.

4.1 Sliding masses

Sliding masses relocate the center of mass of the system. Their operation is based on the movement of a platen, along a fine-threaded rod driven by a stepper motor. The platen weights 0.615 kg and four control pulses (one step) move the mass along the millimetric- threaded rod (M7X1) a total distance of 0.005 mm. The maximum displacement of the platen is 5 cm; this restriction makes necessary that manual balancing locates the platform near the horizontal plane, before automatic control starts. Fig. 10 shows the drawings of a complete sliding mass assembly and the platen, where the nominal centers of mass are depicted.

4.2. Manual balancing procedure

This procedure must be followed independently of the automatic balancing method that will be performed afterwards. Initially the platform is in balance (i.e. the sum of moments is zero) the strategy consists in maintaining the balance, adding a couple of components each time, counteracting mutually the unbalancing effect. As the two elements have different mass, they should be located at different distances from the center of the air-bearing. Following this strategy, more components can be added without altering static equilibrium. As an example, suppose that we have the elements of the balancing system, and all of them are arranged as shown in Fig. 11. In this case, the two sliding masses are counteracted by the batteries located at 21.5 cm from the center, meanwhile the control electronics is equilibrated by the ballast mass in the imaginary circle of radius 24 cm. The electronic compass is located exactly in the center of the table and no counterweight is needed, because it causes the center of mass being located slightly above the geometric center of the air-bearing, giving no noticeable instability to the system.

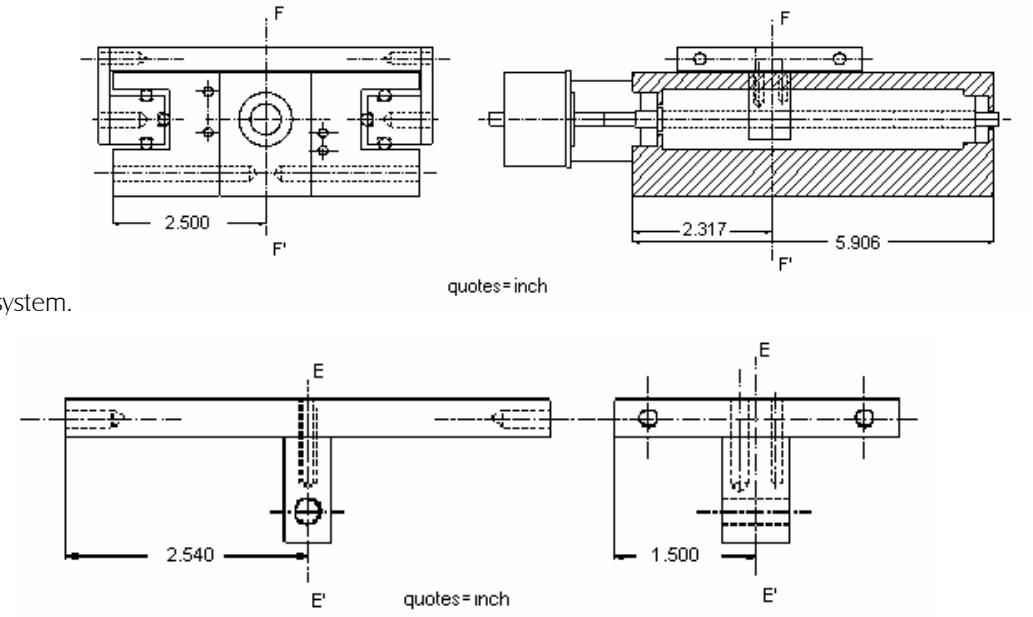

Figure 10. Location of the F-F' and E-E' axis, where the center of gravity of the total moving mass assembly and the platen, respectively, are positioned

The system is reasonably balanced after following the above-mentioned accommodation, however, automatic balancing is necessary to reduce as much as possible the external (gravitational) torques.

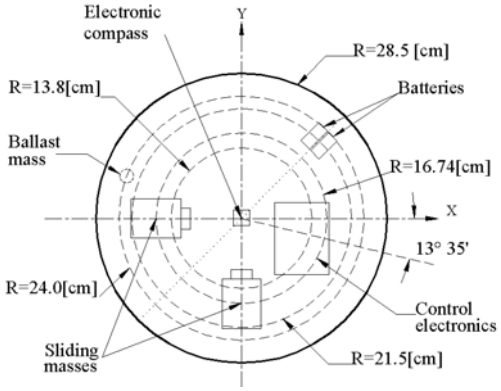

Figure 11. Simulation platform with all the components of the balancing system and the wireless interface located in fixed positions

4.3 First automatic balancing method

The main steps of the procedure, fully described in [32], are as follows: The total mass of the system is calculated. Initial calibration of angular rates and orientation is performed, a torque profile is commanded and data recorded in the onboard computer. Computation of the input-output data gives an estimate of the moment of inertia matrix, as well as the difference between the center of mass (CM) and the center of rotation (CR) of the platform. Sliding masses are moving in three-axis relocating the CM closer to the CR (i.e. the geometrical center of the air-bearing). The process is repeated until the threshold limit is reached (0.025 mm), as shown in Fig. 12. After three iterations the system is balanced with a final residual torque of 50 gr-cm.

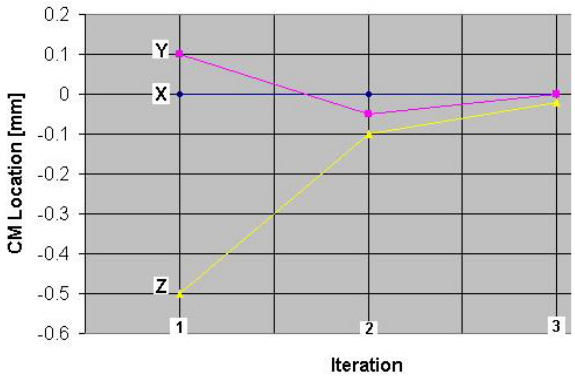

Figure 12. After 3 iterations the system is balanced using the system's identification approach

4.3.1 *Equations of motion*

Euler equations and Euler angles are used to model the dynamics of the spacecraft simulator, with respect to an inertial coordinate system, through the utilization of a rotation matrix (with the sequence ZYX). The common form of the Euler rate equations is also employed

$$\begin{bmatrix} \dot{\psi} \\ \dot{\theta} \\ \dot{\phi} \end{bmatrix} = \begin{bmatrix} 0 & \frac{sen\phi}{\cos\theta} & \frac{\cos\phi}{\cos\theta} \\ 0 & \cos\phi & -sen\phi \\ 1 & sen\phi\tan\theta & \cos\phi\tan\theta \end{bmatrix} \begin{bmatrix} \omega_x \\ \omega_y \\ \omega_z \end{bmatrix}. \quad (1)$$

Ho, the angular momentum vector about the mass center can be written as

$$\mathbf{Ho}=\mathbf{M}(\mathrm{r}\times\mathrm{V}), \tag{2}$$

where M is the total system mass, r is the vector that connects the center of rotation (CR) with the center of mass (CM), and V is the velocity corresponding to the center of mass.

It can be demonstrated that the time derivative of the angular momentum is equal to the applied external forces:

$$\frac{d\mathbf{H_o}}{dt}=\mathbf{M_o}, \tag{3}$$

where Mo is the applied external torque to the platform (i.e. internal, gravitational, and aerodynamic). The time rate of change of the angular momentum can be expanded to

$$\frac{d\mathbf{Ho}}{dt}=(\mathbf{r}\times M\dot{\mathbf{r}})+\dot{\mathbf{H}}_\mathbf{c}+\left[\omega_i\times(\mathbf{r}\times M\dot{\mathbf{r}})\right]+\left(\omega_i+\mathbf{H_c}\right), \tag{4}$$

where Hc is the angular momentum about the CM, and ωi is the angular velocity vector.

Some assumptions must be made for the utilization of equation (4): translational acceleration of the CR is zero, and the platform is a rigid body. The external applied torques, Mo, can be decomposed into

$$\mathbf{MM_o}=\mathbf{M_{internal}}+\mathbf{M_g}+\mathbf{M_{aero}}, \tag{5}$$

where Minternal are the internal torques, Mg is the gravitational torque from the offset CM, and Maero is the aerodynamic drag torque, when the platform is spinning.

The above- mentioned vectors are defined as

$$\mathrm{Hc}=\begin{bmatrix} I_{xx}\omega_x+I_{xy}\omega_y+I_{xz}\omega_z \\ I_{yx}\omega_x+I_{yy}\omega_y+I_{yz}\omega_z \\ I_{zxx}\omega_x+I_{zy}\omega_y+I_{zz}\omega_z \end{bmatrix}, \tag{6}$$

$$\mathrm{Minternal}=\begin{bmatrix} M_{\mathrm{int}\,x} \\ M_{\mathrm{int}\,y} \\ M_{\mathrm{int}\,z} \end{bmatrix}, \tag{7}$$

$$\mathrm{Maero}=\begin{bmatrix} -B_x\omega_x^2 \\ -B_y\omega_y^2 \\ -B_z\omega_z^2 \end{bmatrix}, \tag{8}$$

$$\mathrm{Mg}=\mathrm{M}^*\mathrm{g}^*\begin{bmatrix} 0 & -\cos\phi\cos\theta & sen\phi\cos\theta \\ \cos\phi\cos\theta & 0 & sen\theta \\ -sen\phi\cos\theta & sen\theta & 0 \end{bmatrix}r. \tag{9}$$

Substituting equations (4) and (5) into (3) together with the above definitions, yields an equation of the form

$$\mathbf{A}\dot{\omega}+\mathbf{B}=\mathbf{M}. \tag{10}$$

Rearranging we have:

$$\dot{\omega} = (\mathrm{A})^{-1}(\mathrm{M} - \mathrm{B}), \tag{11}$$

Equations (11) and (1), integrated and solved simultaneously with the rotation matrix describes the dynamics of the simulator. Moreover, equation (11) can be greatly simplified. If we assume that ω, r, Maero, and the cross products of inertia are small compared with the other terms, and Minternal is zero, then we have

$$\dot{\omega} = \begin{bmatrix} [mg / I_{xx}](-r_y \cos\phi\cos\theta + r_z sen\phi\cos\theta) \\ [mg / I_{yy}](r_x \cos\phi\cos\theta + r_z sen\theta) \\ [mg / I_{zz}](-r_x sen\phi\cos\theta - r_y sen\theta) \end{bmatrix}. \tag{12}$$

The platform was modeled like a rigid body whose center of mass is shifted a distance r with respect to the center of rotation of the air-bearing.

4.4 Second automatic balancing method

Static equilibrium exists when the simulation platform is perfectly horizontal. The basis for this assumption is that any existing torque is jointly actuating in the center of mass of the system. A very practical balancing procedure was developed to equilibrate the table in the pitch and roll axis i.e. the local horizontal plane. The yaw axe is manually adjusted with a threaded counterweight

4.4.1 *Two-axis balancing*

A proportional automatic control scheme was implemented. Input signals, coming from the two inclinometers, are compared against the threshold reference limit of ± 0.25 arc deg. If platform's orientation is out of this range then a sequence of pulses, proportional to the magnitude of the displacement, is executed. Sliding masses are displaced taking theplatform to a new position. The process continues until the desired orientation is reached. Three-axis attitude is transmitted 12 times per second by the radio link and received by the monitoring system for data display and storage (see Fig. 13).

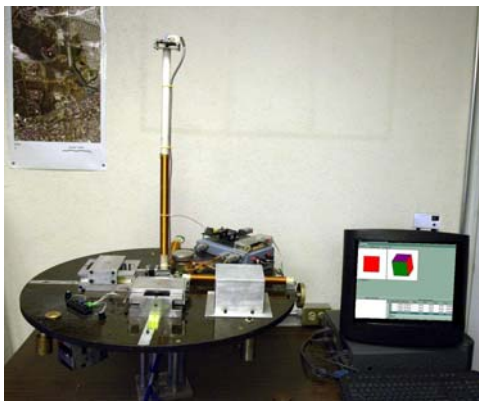

Figure 13. Monitoring process of the small satellite attitude control simulator, during an automatic balancing procedure

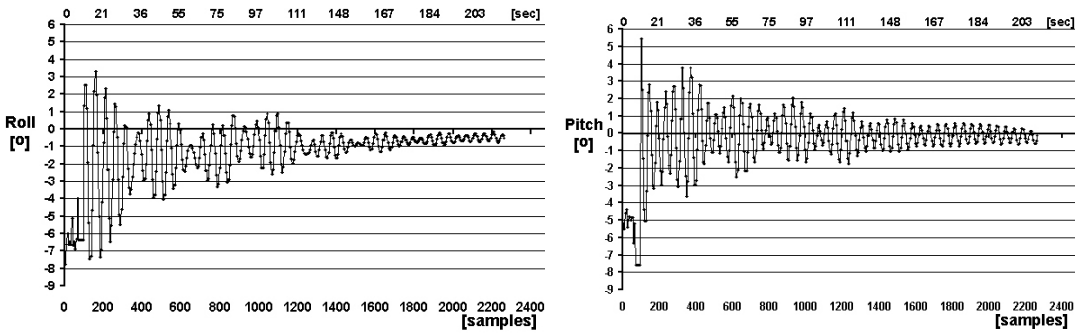

Figure 14. Automatic balancing tests performed in the roll and pitch axis, respectively

The graphics on Fig. 14 depicts a typical example that demonstrates the effectiveness of the control system in the execution of the automatic balancing procedure. Beginning with a deviation of –7 deg in roll, and –5 in pitch, platform's deviation was driven into the threshold limit. Graphics were constructed from 2,200 data samples, performing approximately 3 minutes of iterations, until the system reached a steady state.

4.5 Oscillating period as a measure of balancing, and final residual torques

The effectiveness of the automatic balancing procedure can be best estimated by the increment in the oscillation period of the simulator [27]. It was evaluated at different balancing threshold limits: ± 3, ± 2, ±1, ±0.5 and ± 0.25 arc deg. The importance of a good balance is in direct relationship with the attitude control, and the energy: the most critical resource in small satellites. Careful energy budget design, based into accurate ground experimentation, will assure mission success in space. It is recommended to maintain the residual torques at least two orders of magnitude below the maximum control torque available in the spacecraft [10], and this last, must be one order of magnitude greater than the maximum disturbing torques expected in orbit [34]. The graphic on Fig. 15 shows the magnitudes of the disturbing and control torques for a cubic shape satellite, 50 kg of mass, 0.5 m by side, and orbiting at 780 km with an inclination of 89 arc-deg. The torque produced by the momentum/reaction wheels is three orders of magnitude bigger than the torque produced by gravity-gradient; and the one generated by the magnetic coils, will be enough for backup control purposes.

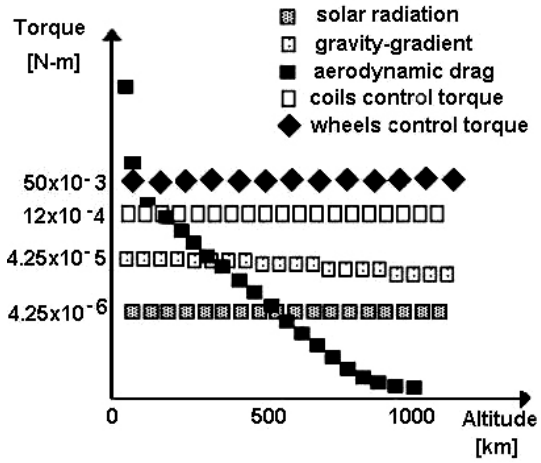

Figure 15. Disturbing and control torques for a satellite orbiting at 780 km height

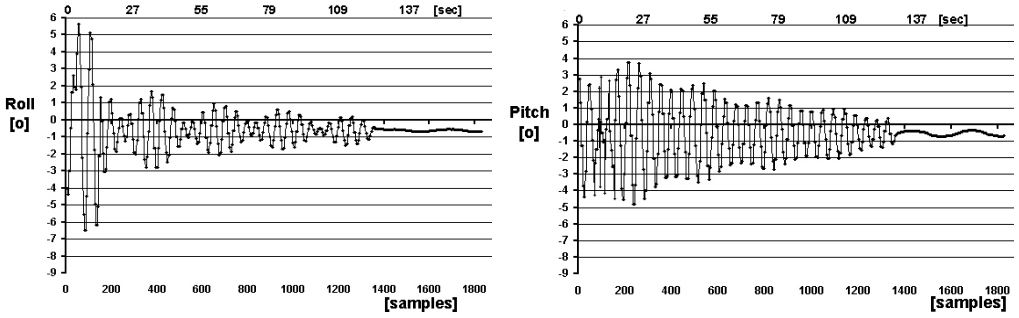

Figure 16. Roll and pitch axis oscillation, once the platform was balanced

Fig. 16 shows an oscillation test over the roll and pitch axis, once automatic balancing was performed in the platform. Fig. 17 resumes the period values for different threshold limits. When threshold grows; the oscillation period diminishes.

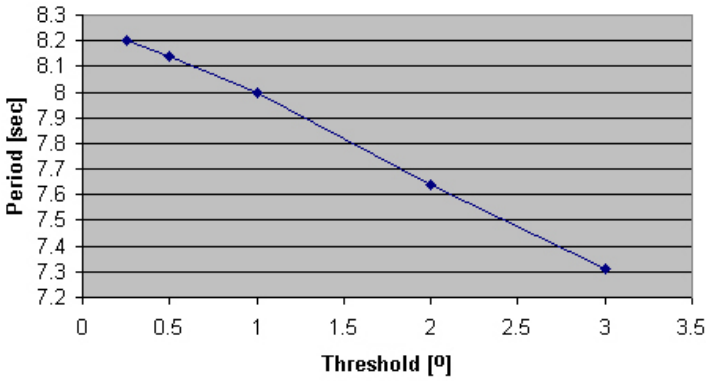

Figure 17. Threshold limits vs. oscillation period

4.6 Discussion

With the first balancing method, presented in condensed form in this paper, a residual torque of 50 gr-cm was achieved. This result was very similar to that obtained by Young [31] using the same kind of low-cost (20K USD) simulator [8]. In the second procedure, a final residual torque of 20 gr-cm was obtained while reducing 43% the mass of the balancing system; this is significative as well as the simplification in the methodology. In more sophisticated and expensive systems (200-400K USD) like those described by Rizos et. al. [35], and De la More et. al. [36]; residual torques range from 1 to 5 gr-cm. The good result obtained in our spacecraft simulator was reached mainly due to

- The enhanced resolution the newly designed mass movement assemblies can handle (driven to the maximum achievable resolution of ± 0.25 [arc deg]).
- Carbon fiber composites utilization in the table construction, because, elongations and contractions due to temperature changes (of 1C) were reduced from 0.0095 mm/C, using a similar-size aluminum platform, against 0.00001064 mm/C; resulting in a reduction from 38 gr-cm to 0.042 gr-cm, respectively. This is particularly important when air currents produce differential temperatures along the surface of the table.
- The careful machining of the air-bearing, resulting in a deviation of 0.032 mm from a nominal sphere.

5. CONTROL TESTS

In this section some experimental results with magnetic coils and inertial wheels are presented. Straightforward control laws were implemented with the purpose to evaluate the functionality of the spacecraft simulator, simultaneously with all of the subsystems. Fig. 18 shows the results of two control maneuvers with a magnetic coil as actuator. The platform was initially with a deviation of +53 and -65 arc deg in the Yaw axe, respectively, and the attitude corrected by the proportional-control algorithm. The actuator interacted with the geomagnetic field and the desired attitude was reached.

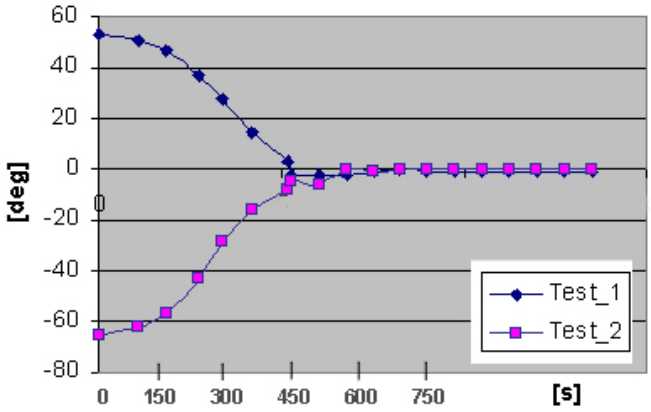

Figure 18. Two control maneuvers in the yaw axe, with a magnetic coil as actuator

Fig. 19 shows the response inertial wheels can deliver in the presence of important deviations in the simulator, this allows for fast pointing maneuvering, as expected.

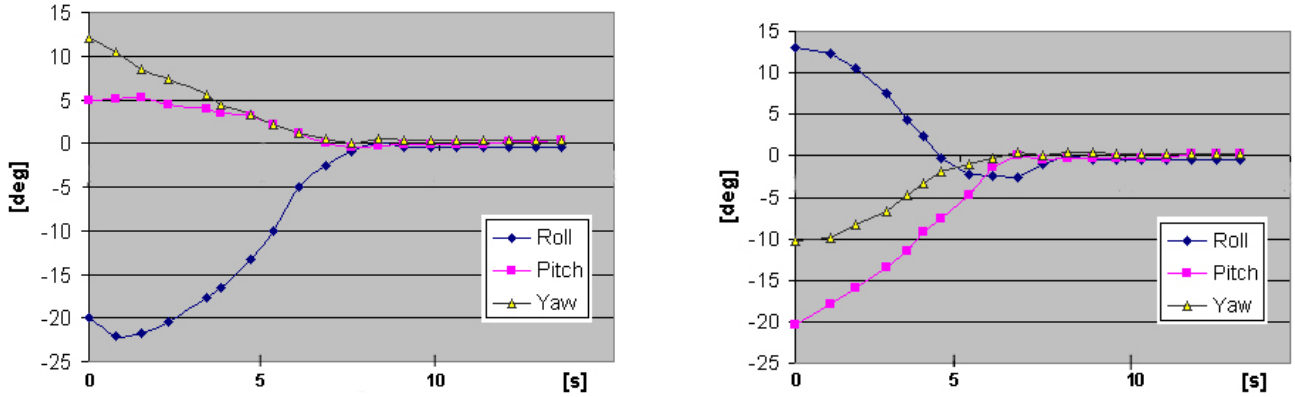

Figure 19. Experimental results for two different initial conditions with the inertial wheels as actuators

6. CONCLUSIONS

This paper resumes the work of many years of development of a facility that will be used to educate future generations of attitude dynamics and control engineers. Many components were homemade: Sun and Earth sensors, inertial measurement unit, magnetic coils, three-axis air-bearing, and the onboard computer. Sensors and actuators were fully modeled and characterized, and a methodology for moment of inertia matrix determination of the platform was developed, for both: balancing and control purposes. Two different balancing approaches were embraced and a very practical balancing technique was developed taking advantage of available resources on the spacecraft simulator. It was proved that it is possible to carry out static balancing, maintaining the forces actuating only over a plane, reaching equilibrium on the platform. The automatic static balancing system allows important savings in space, mass, and complexity compared with the previously developed dynamically balancing system [32]. Final residual torque in the simplified method was 20 gr-cm against the 50 gr-cm obtained with the former, with 43% in mass savings. This is considered a very good result tacking into account that a low-cost spacecraft simulator was constructed. A monitoring system was developed for post-processing analysis. Attitude data are displayed and stored 12 times per second, allowing attitude control and stabilization sensors, actuators and algorithms being properly evaluated. Some control tests were carried out with the purpose to assess different control stabilization techniques, without the interference of significative gravitational torques.

7. REFERENCES.

Favor de cambiar la ubicación de nombres

[1]. Stanton. J., Navy, Air Force to Develop Twin-Mirror Laser-Retargeting Satellite Technology. National Defense Magazine, August 2002.

[2]. Wang, P., Hadaegh, F.Y. and Lau., K. Synchronized formation rotation and attitude control of multiple free flying spacecraft. J. Guidance Control & Dynamics. Vol 22, no. 1, 1999. pp28-35.

[3]. Lau., K. Colavita, M., Blackwood, G. L.R.M. Shao, and D. Gallagher., The new millennium formation flying optical interferometer. Proc. of AIAA GNC Conference. New Orleans, LA. paper AIAA 97-3820,. pp. 650-656, 1997.

[4]. Kim B.M., Velenis E., Kriengsiri P. and Tsiotras P., Designing a low-cost spacecraft simulator. IEEE Control Systems Magazine. 2003 pp 26-37.

[5]. Roe F.D, et. al., Simulation Techniques for Avionics Systems- An Introduction to World Class Facility. Proc. of AIAA Flight Simulation Technologies Conference, no. 96-3535, (San Diego, California), 1996. pp. 535-543.

[6]. Shaviv, G. and Shachar, M., TechSAT-1, An Earth pointing, three-axis stabilized microsatellite. Space Technology. vol 15, No. 4. 1995 pp245-256.

[7]. Schwartz J.L, Peck M.A and Hall C.D., Historical review of air-bearing spacecraft simulators. J. of Guidance Control & Dynamics. 2003. Vol 26, no 4. pp 513-522.

[8]. Fullmer et al., The Development of a Small Satellite Attitude Control Simulator. 6th. Annual AIAA-USU Conference on Small satellites. Logan, Utah. 1992 September. pp 1-14

[9]. Prado J., Peralta-Higuera A., Navarrete M., Bisiacchi G., Simulador Físico para Prueba de Sistemas de Detección de Orientación de Satélites, en un Medio sin Fricción. SOMI XII Cong. Nal. de Inst. S L P. México. Memorias del Cong. 1997. pp738-742.

[10]. Haussermann W. and Kennel H., A Satellite Motion Simulator. Astronautics Vol 5 No. 12 December 1960. pp 22-23 and 90-91.

[11]. Juárez A., Balanceo automático de un simulador para control de orientación de satélites. Tesis de Licenciatura, Facultad de Ingeniería, UNAM. 2001. pp1-76.

[12]. ICSENSORS Technical notes. Accelerometer model 3140. Milpitas, Cal. U.S.A. 1999

[13]. SYSTRON DONNER GyroChip II Solid State Rotation Sensor. U.S.A. 1999.

[14]. ADVANCED ORIENTATION SYSTEMS Ez-Compass-3 Application Manual. Linden, NJ. USA. 1999

[15]. Prado J., Bisiacchi., Ruiz D., Construcción y Calibración de un Sensor de Sol para Aplicación Espacial. SOMI XVII Cong. Nal de Inst. Mérida, Yuc. México, Memorias en CD. 2002. pp1-12. Trabajo ELECTRO36.

[16]. OPTOELECTRONICS OTC-11-5 series, single stage, thermoelectrically cooled lead selenide detectors datasheet. Petaluma, Cal. USA. 1985.

[17].- Prado J., Miranda V., Corona A., Sensor de tierra para detección de orientación de un satélite. SOMI XII Cong. Nal de Inst. SLP. México. Memorias del Cong. 1997 pp 743-747

[18]. Espinosa A. G., Salgado G., Implementación de un sistema de control de orientación para un satélite pequeño, utilizando ruedas inerciales. Tesis de Licenciatura. Ingeniería Electrónica. Facultad de Estudios Superiores Aragón, UNAM. 2002

[19]. Schmidt, E. Jr., The application of magnetic attitude control to a momentum biased synchronous communications satellite. AIAA Guidance and control conference. Boston, Massachusetts. 1975 August. AIAA paper No.75-1055

[20]. Bar-Itzhack, I.Y. and Shorshi, I.Y., Near Earth orbit determination using magnetometers. Proc. First ESA Int. Conf. On Spacecraft Guidance, Navigation and Control Systems. ESTEC, Noordwijk, The Netherlands, 1991, June 4-7.

[21]. Juárez G., Utilización de bobinas magnéticas para control de orientación de satélites pequeños. Tesis de Licenciatura. Ingeniería Electrónica. Facultad de Ingeniería, UNAM. 1999 pp 1- 62

[22]. Carrasco F., Pruebas de control de estabilización para un satélite pequeño empleando bobinas magnéticas y ruedas inerciales. Tesis de Licenciatura. Ingeniería Electrónica. Facultad de Ingeniería, UNAM. 2004. pp 1- 86

[23]. LINX TECHNOLOGIES Ref. Manual, HP-II module. Ashley Place, USA. 2001

[24]. Mesinas M., Sistema de monitoreo de un simulador para control de orientación de satélites. Tesis de Licenciatura. Ingeniería Electrónica. Fac. de Ing., UNAM. . 2002. pp 76.

[25]. M68HC11, Reference Manual. Motorola. U.S.A., 1991.

[26]. Vicente-Vivas E., et al., Space Qualified Computer Server Developed for Long Life Microsatellite Applications. Research On Computer Science, Vol.9, pp. 25-35, CIC-IPN, México, DF, 2004, Sept.

[27]. Olsen T., Design of an Adaptive Balancing Scheme for the Small Satellite Attitude Control Simulator (SACCS). Master Thesis, Utah State University. 1995

[28]. Tuley G. W. And García J., A state of the art mass properties laboratory, Mc Donnell Douglas Helicopter Company. 48th Annual Conference of Society of Allied Weight Engineers, Inc. Alexandria, Virginia. 1989, May 22-24 . SAWE paper No. 1883.

[29]. Lang, W., Triaxial Balancing Techniques (A Study of Spacecraft Balance with Respect to Multiple Axes). Greenbelt, MD. NASA Goddard Space Flight Center.TN D-2144.

[30].- Mangus J.A., Passarello, and Van Karsen., Estimating rigid body properties from force reaction measurements. 11th Int. Modal Analysis Conf. Kissimmee, FL. 1993, pp469-472.

[31].- Young J.S., Development of an automatic balancing system for a small satellite attitude control simulator (SSACS). Master thesis. Utah State University, 1998.

[32]. Prado J., Bisiacchi G., Dynamic Balancing for a Satellite Attitude Control Simulator. Instrumentation and Development. Journal of the Mexican Society of Instrumentation. SOMI. Vol 4. No 5. 2000. pp 76-81.

[33].- Prado J., Bisiacchi G., Mesinas M., Ruiz D., Sistema de Monitoreo Inalámbrico de un Simulador Para Control de Orientación de Satélites. SOMI XVII Cong. Nal. de Inst. Mérida, Yuc. México. Memorias en CD. 2002. pp1-12. Trabajo ELECTRO35.

[34].- Wertz JR. (Editor). Spacecraft Attitude Determination and Control. Kluwer Publishers, The Netherlands. 1990

[35].- Rizos I, Arbes J and Raoult J.C., A Spherical Air-Bearing-Supported Test Facility for Performance Testing of Satellite Attitude Control Systems. ESRO-CR66, also 4th. IFAC Symposium. Dubrovnic, Yugoslavia. 1971, Sept. 6-10.

[36]. De More L.A. et. al., Design study for a high-accuracy three-axis test table. J. of Guidance Control & Dynamics. Vol 10 No. 1, 1987 Jan-Feb. pp104-114.